Journal of Food Legumes
38(1): 94-107, 2025
DOI: 10.59797/jfl.v38.i1.247

Research Paper

Drying method induced structural and functional attributes of mungbean protein

Srishti Upadhyay[1], Vijay Singh Sharanagat[1]*, Gourav Chakraborty[1] and Jeeva Kiran Banoth[1]

[1]*Department of Food Engineering, National Institute of Food Technology Entrepreneurship and Management, Kundli, HR -131 028, India*

***Corresponding author e-mail:** vijaysinghs42@gmail.com*

***Received:** November 6, 2024*
***Accepted:** December 17, 2024*

ABSTRACT

In this study, mungbean protein (MBP) was extracted via alkaline extraction and isoelectric precipitation, and the effects of freeze-drying (FD) and spray-drying (SD) on its physicochemical, functional, rheological, thermal, and nutritional properties were analyzed. Spray-dried MBP (SDMBP) demonstrated higher solubility (72.52%), emulsifying activity (32.26%), and stability indices (34.32%), making it highly suitable for various food applications such as mayonnaise, emulsion, functional beverages, and 3-D food printing. Whereas, the freeze-dried MBP (FDMBP) exhibited higher water and oil holding capacities, making it ideal for formulations requiring moisture and fat retention, such as plant-based meat analogs, baked goods, and dairy alternatives. Structurally, FDMBP exhibited higher free sulfhydryl, total sulfhydryl, and disulfide bonds, alongside lower turbidity, reflecting better protein integrity. Thermal properties revealed denaturation temperatures of 100.9°C, 107.2°C, and 153.3°C for MBF, SDMBP, and FDMBP, respectively, with corresponding enthalpy changes of 26.03 J/g, 24.38 J/g, and 19.9 J/g. Thermogravimetric analysis (TGA) indicated degradation onset at 240°C for MBF, and 266°C for SDMBP and FDMBP, highlighting their thermal stability for high-temperature processing. All the samples exhibited shear-thinning behavior, with SDMBP showing the highest viscosity and a gelation temperature of 82°C underscoring its potential for thickening and gelling applications. FDMBP's showed higher retention of essential amino acids due to their low-temperature processing, enhancing its nutritional profile for health-focused formulations. Whereas both methods yielded high levels of aspartic and glutamic acids which are beneficial for flavor enhancement. These findings underscore the advantages of freeze-drying for nutritional preservation and spray-drying for functional enhancements.

Key words: Mungbean, Protein, Drying, Spray-drying, Freeze-drying

INTRODUCTION

The rising consumer interest in plant-based diets, fueled by health concerns, ethical considerations, and environmental awareness, has led to a significant surge in demand for plant-based foods and proteins. Plant proteins provide a sustainable alternative to animal-based sources, contributing substantially to the global protein supply while minimizing the environmental impact associated with livestock production (Özdemir *et al.* 2022). Legumes and nuts, recognized for their protein-rich profiles and lower greenhouse gas emissions, are increasingly viewed as viable protein sources compared to traditional dairy and meat products (Ritchie *et al*. 2022). Among these plant-based options, mungbean (*Vigna radiata*) has emerged as a particularly notable legume due to its high protein content, which ranges from 21.0% to 31.3%, and its rich profile of essential micronutrients (Jeong and Cho 2024).

Mungbean protein (MBP) is distinguished by its favorable amino acid profile, surpassing the nutritional standards set by the FAO/WHO. Its high digestibility and cost-effectiveness further enhance its appeal for use in various food and nutraceutical applications (Dahiya *et al.* 2015). Recent studies have highlighted the diverse applications of MBP in the food processing sector, including its incorporation into plant-based meat analogs (PBMAs) and dairy substitutes. For instance, research has demonstrated that MBP can be effectively utilized in the formulation of PBMAs, which aim to replicate the texture and flavor profiles of traditional meat products. These analogs are crucial for meeting the dietary needs of

consumers transitioning to plant-based diets while offering a more sustainable food choice.

In addition to PBMAs, the development of plant-based dairy analogs (PBDAs) using mungbean protein has also gained traction (Brishti *et al*. 2017). For example, studies have shown that mungbean-based yogurts exhibit improved textural properties compared to those made from other plant proteins, indicating MBP's potential in creating high-quality dairy alternatives (Yang *et al*. 2021). Furthermore, the increasing interest in innovative food production methods has led to the exploration of three-dimensional (3D) printing techniques in the manufacturing of plant-based products (Chao *et al*. 2024).

Despite the promising applications of MBP in the food processing sector, there remains a notable lack of research examining the impact of various drying methods on the physicochemical and functional properties of mungbean protein isolates. Freeze-drying and spray-drying are the predominant methods used for drying protein. Freeze-drying preserves nutrients effectively whereas the high costs of energy consumption and higher drying time limit its industrial use. Conversely, spray drying is favored for its rapid dehydration, cost-effectiveness, and control over particle size, shape, and morphology. Additionally, the high temperature used in spray drying enhances the functional properties of protein. The choice of drying method can significantly influence the characteristics and quality attributes of the protein, thereby affecting its potential applications in functional foods (Nie *et al.* 2023, Shen *et al.* 2021). Therefore, this study aims to fill this research gap by investigating the effects of different drying techniques, specifically spray-drying and freeze-drying, on the properties of MBP and comparing these isolates to mungbean flour. Through this investigation, we seek to provide valuable insights into the optimization of MBP for diverse applications in the food industry, particularly in the burgeoning field of plant-based alternatives.

MATERIALS AND METHODS

Material collection

Mungbean (Brand Tata) was purchased from Amazon India. The mungbean grains were cleaned, grounded, sieved (180 um sieves), and packed for further analysis. Soyabean oil was purchased from Fortune Ltd. All the other chemical reagents and solvents used were of analytical grade.

Ultrasound-assisted alkaline extraction of MBP

The extraction of protein from mungbean flour (MBF) was performed using the method of Jeong and Cho (2024), with slight modifications. In brief, the MBF was dispersed in distilled water (1:5, w:v) and thoroughly mixed (2 h) using the magnetic stirrer (RH Basic 1, IKA, Germany). The pH of the prepared dispersion was adjusted to 9 (using 1 M NaOH), and ultrasonication (US, 15 min) (ULTRA-PS, Ultra Autosonic India Pune, India) was performed for the complete dissolution of protein. The obtained solution was centrifuged at 7000*g for 15 min (Sigma 3-18KS, Germany), and the supernatant was collected. Subsequently, the pH of the supernatant was changed to 4.5 using 1 M HCl to facilitate the precipitation of protein, and the obtained solution was centrifuged (9000*g, 10 min). After centrifugation, the precipitate was collected, washed with distilled water (three times), and the solution was neutralized. The prepared solution was dried using the freeze-drying and spray-drying methods separately.

For freeze-drying, the sample solution was lyophilized at -80 °C and dried at -40 °C using the lab scale freeze dryer (Model H-T40m-P, Beijer, TAIWAN). The freeze-dried samples were pulverized using a mortar pestle, sieved (mesh No. 40), and packed for further analysis. The spray drying of the extracted protein solution was performed using a lab-scale spray dryer (SS-316L, SPRAYMAT, Jay Instruments & Systems Pvt. Ltd., Mumbai, India). The spray drying parameters, i.e., Inlet temperature (170 °C), outlet temperature (80 °C), and feed rate (6.5 mL/min), were set, and solution concentration was adjusted to 6.5 Brix using the distilled water.

Characterization of the MBF and protein isolate protein content, extraction yield and turbidity

The protein content (%) of the mungbean flour (MBF), freeze-dried mungbean protein (FDMBP), and spray-dried mungbean protein (SDMBP) isolates was determined using Kjeldahl Apparatus (K-439, Buchi, Mumbai, India), and the protein content was calculated according to the standard Kjeldahl method (AOAC 2016). The protein extraction yield (Freeze drying -45.85% and Spray drying -38.25 %) was calculated using Equation 1 (Wintersohle *et al*. 2023).

$$\text{Protein extraction yield (\%)} = \frac{\text{Protein content in protein isolate(\%)} X \text{Weight of isolate(g)} X 100}{\text{Protein content in flour(\%)} X \text{ Weight of flour(g)}} \quad \ldots(1)$$

Turbidity of the protein and flour (1mg/mL) was measured using UV/VIS spectrophotometer (UV3092, LabIndia, Mumbai, India) at 600 nm absorbance using the method of Nahimana *et al.* (2024).

Color analysis, particle size, and contact angle

The color analysis of flour and protein samples was performed using a handheld Chromameter (CR-400, Konica Minolta Optics, Japan), as described by Chen *et al*. (2012). The particle size of flour and protein samples was determined using the particle size analyzer (PSA 1090, Anton Paar, Austria). In brief, the distilled water was filled in the liquid flow assembly and the sample was dispersed in distilled water to obtain the obscuration range of 5-30%. The particle size of the samples was recorded in the statistical form i.e. D10, D50, and D90 showing total percentiles of particles below 10%, 50%, and 90%, respectively.

The three-phase contact angle (oil-water-solid) was obtained using Kruss-DSA25E (Germany). Thin slices of MBF, FDMBP, and SDMBP, each with a diameter of 15 mm and a thickness of 2 mm, were prepared via a hydraulic press operating at 30 MPa (Kou *et al.* 2023). These slices were placed within a rectangular optical glass cell containing the oil phase. Subsequently, a 10 µL water droplet was carefully dispensed onto the slice surface using a syringe. Analysis of the three-phase contact angles was conducted using ImageJ software.

Sulfhydryl group and disulfide groups

The sulfhydryl group and disulfide groups present in flour and protein samples were determined using the method of Brishti *et al.* (2020). For the sulfhydryl group, 30 mg of protein sample was dispersed in 10 mL Tris-Glycine Buffer with (total SH) and without (free SH) 8 M Urea followed by mixing of 0.1 mL of Ellman's reagent [5,5′-dithiobis-(2-nitrobenzoic acid) in Tris-Glycine buffer and 4 mg/mL, pH 8.0]. The solution was incubated in the dark with continuous stirring (150 rpm) for 1 h and centrifuged at 7500*g for 10 min. The supernatant of samples with and without 8 M urea was collected to find free and total SH.

For disulfide bonds, 30 mg of protein sample was dispersed in 10 mL Tris-Glycine Buffer (10 M) added with 0.03 mL of β-mercaptoethanol. The solution was incubated in the dark with stirring for 1 h, followed by the addition of 10 mL of trichloroacetic acid (12%) and further incubation in the dark (1h) under continuous stirring. The incubated mixture was centrifuged at 5000*g (10 min) and the precipitate was collected. The 3 mL of Tris-Glycine buffer 8 M urea and 0.04 mL of Ellman's reagent [DNTB 5, 5′-dithiobis-(2-nitrobenzoic acid) was added in precipitate, incubated (30 min) and further centrifuged at 7500*g (10 min). The sample absorbance was recorded at 412 nm against the blank, and the sulfhydryl group and disulfide bonds were determined using the following equations 2 and 3, respectively.

$$\mu \text{ mol SH/g} = \frac{73.53 \, X \, A \, X \, D}{C} \quad \ldots(2)$$

$$\mu \text{ mol SS/g} = \left(\frac{73.53 \, X \, A \, X \, D}{C} - \text{SH}_{\text{free}} \right)/2 \quad \ldots(3)$$

where A, C, and D, are absorbance at 412 nm, concentration of the sample (mg/mL), and dilution factor, respectively.

Surface hydrophobicity (H_o)

Surface hydrophobicity (Ho) was measured using the Coomassie Brilliant Blue G-250 (CBBG) dye binding protocol as described by Kamboj *et al.* (2024). Briefly, 1.2 mL of sample (5 mg/mL) was mixed with 300 µL of CBBG dye solution (0.1 mg/mL). The obtained solution was vortexed for 3 min and thereafter centrifuged for 2000*g (10 min). The resultant supernatant was again centrifuged (2000g, 10 min) and absorbance of the obtained supernatant was observed at 585 nm using a UV/VIS spectrophotometer (UV3092, LAB INDIA, Mumbai, INDIA). The CBCG-bound Ho was calculated using equation 4.

$$\text{CBCG(bound)} = 30 \text{ µg } X \frac{\text{Acontrol} - \text{Asample}}{\text{Acontrol}} \quad \ldots(4)$$

Where A = absorption at 585 nm

Functional properties

Protein solubility (PS)

The PS of MBF, FDMBP, and SDMBP samples was determined using a UV/VIS spectrophotometer (UV3092, LAB INDIA, Mumbai, India) following the method of Jeong et al. (2024), with slight modification. The samples were dispersed in distilled water (1% w/v) and pH was adjusted to 7, followed by mixing in a rotary shaker (600 rpm, 60 min). After mixing, samples were centrifuged (10,000*g, 30 min, 20 °C) and the supernatant was collected. The protein content was determined by

taking the absorbance of the supernatant at 660 nm using a standard curve (y = 0.7162x + 0.1286, R2 > 0.998) generated by bovine serum albumin (BSA) as mentioned in equation 5.

$$PS = \frac{Csupernatant}{Ctotal\ X\ \%Protein\ content} \quad \ldots(5)$$

Where, $C_{Supernatant}$ - Concentration of protein in supernatant, C_{Total} - Initial amount of protein or flour.

Emulsifying activity (EAI) and stability index (ESI)

The EAI and ESI of flour and protein samples were determined using the protocol described by Brishti et al. (2020).

Water (WHC) and oil holding capacity (OHC)

WHC and OHC of flour and protein samples were determined by following the method outlined by Jeong and Cho *et al*. (2024) and Özdemir *et al*. (2022), respectively.

In-vitro protein digestibility

The simulated static in-vitro gastrointestinal digestion was performed using gastric and intestinal solutions of porcine pepsin and pancreatic enzymes, respectively. A 10 mL sample dispersion (1:10 sample to water) was prepared and mixed with 7.5 mL of simulated gastric fluid and 1.6 mL of porcine pepsin followed by volume make up to 20 mL using the distilled water. The prepared sample solution pH was changed to 3 using 1 M HCl and incubated for 2 h at 37°C. After incubation, the sample was heated to 90°C (10 min) in a hot water bath to terminate the enzymatic reaction. Thereafter, 11 mL of SIF, 5 mL of pancreatic enzyme, 2.5 mL of fresh bile salt, and 40 µL of $CaCl_2$ (0.3 M) were added and the volume was made to 40 mL using distilled water. The pH of the prepared solution was changed to 7 and incubated at 37 °C for 2 h. The 12% trichloroacetic acid (TCA) solution was added to the mixture and the supernatant was collected to determine the non-protein nitrogen (NPN) using the Kjeldahl method. The percent protein digestibility was calculated using the following equation 6.

$$\text{Protein digestability}(\%) = \frac{NPNafter - NPNbefore - NPNblank}{TNbefore} X\ 100 \quad \ldots(6)$$

NPN_{after} = NPN of GI digesta, NPN_{before} = NPN of sample, NPN_{blank} = NPN of enzyme blank, TN_{before} = Total nitrogen content of respective samples

Surface Morphology, FTIR analysis, and thermal analysis

The surface morphology of flour and protein samples was recorded using the scanning electron microscope under an accelerating potential of 15 kV (JSM 6300 SEM, JEOL, Japan). The samples were directly deposited on aluminum stubs using double-sided carbon conductive tape and were coated with a gold layer with the help of gold sputter. The surface roughness graphs were generated using ImageJ software.

Fourier transform infrared (FTIR) spectra of flour and protein samples were recorded using FTIR Spectrometer (ALPHA, Bruker, Germany). The powdered samples were directly placed over the ATR plate and scanned in the wavenumber range of 400–4000 cm−1 (4 cm−1, 24 Scan). The ATR plate was properly cleaned and the background scan was measured before each analysis. The secondary structures of the MBP isolate were obtained using the FTIR spectrum (Brishti *et al.,* 2020). The secondary structure was determined by using Fourier self-deconvolution on the second derivative function of the amide I region (1600–1700 cm^{-1}) by Gaussian curve-fitting using OriginLab software (OriginLab Corporation, Massachusetts, USA).

The thermal behavior of flour and its protein was obtained by differential scanning calorimeter (DSC 200F3, Netzsch, Germany) and thermo-gravimetric analyzer (TGA209F1D-0072-L, NETZSCH, Germany) by following the method outlined by Barbana and Boye (2013), with slight modification. DSC and TGA analysis were performed in the temperature range of 25 to 300°C (10°C/min) and 40 to 750°C (10°C/min), respectively. All the experiments were performed in an inert environment (N_2 gas).

Rheological analysis

The rheological analysis of MBF, FDMBP, and SDMBP was performed using the MCR 52 rheometer (Anton Paar, Austria). Steady-state and temperature sweep tests were performed using the method of Resch *et al*. (2004), with slight modification. The sample suspensions (14% w/v) were prepared in the distilled water. The steady-state rheology was performed at the share rate of 0.1-100 s−1 (25°C). The temperature sweep test was performed in the temperature range of 25- 95 °C to obtain the G′ and G″ values, and the gelation temperature and time. The temperature sweep test was performed at a constant frequency (1 Hz) and shear stress (1 Pa) in

a linear viscoelastic range.

Amino acid profile

For Amino acid profiling, protein hydrolysis was carried out by adding 5–6 mg of biomass to 10 mL of 6 N HCl. A crystal of phenol was added to the vial, which was then vacuum-dried at 110 °C for 20 hours. The hydrolyzed samples were derivatized using a borate buffer (pH 8.2–10) and the AccQ Tag Fluor reagent (WAT052880), following the protocol outlined in the Waters AccQ Tag method manual (Waters Millipore Corporation, USA, 1993). Detection was conducted using an AccQ-Tag (Nova-Pak C18) 3.9 × 150 mm × 4 µM silica bonded column (WAT052885) with a binary gradient HPLC-FLD system (Waters Corporation, USA). A reference standard containing 16 amino acids (WAT088122) was used to construct a calibration curve ranging from 0.02 to 0.5 µmole L^{-1}.

Statistical Analysis

All the analyses were conducted in triplicates and results were reported as mean ± standard deviation. The data analysis was performed using one-way analysis of variance (ANOVA) in SPSS ($p < 0.05$). The correlation plot was obtained from origin pro 2024b (Learning edition) (MA, USA).

RESULTS AND DISCUSSION

Protein content, turbidity, color, and particle size

The protein content, turbidity, color, and particle size of MBF, SDMBP, and FDMBP samples are depicted in Figure 2A, Table 1, Figure 2C, and Figure 2B. The protein content MBF was 23.33%, and the maximum recovery of protein was observed in FDMBP. The SDMBP isolate (63.75%) was found to have less protein content compared to the FDMBP isolate (66.86%), which might be associated with the difference in drying temperature used in each method. Additionally, the reduction in protein content in spray drying was associated with a heat-induced Maillard reaction, causing complex reactions between amino acids and carbohydrates, thus reducing the protein content. Brishti *et al.* (2020) reported that the formation of tannin-protein complexes in the high heat-drying process was one of the reasons for the reduced protein content in SDMBP. Findings were also supported by Li et al. (2022), who reported the reduction in protein content in spray drying of protein isolate recovered from Rana chensinensis. Turbidity measurement revealed that MBF had higher turbidity compared to FDMBP and SDMBP. The higher turbidity in MBF was associated with the aggregation of powder particles and the presence of higher concentrations of other components like starch and fiber in the flour, which scatter the light and increase turbidity. The turbidity of SDMBP was higher compared to FDMBP which is associated with protein denaturation and aggregation during spray-drying processes (Nahimana *et al*. 2024).

The color properties of the MBF, SDMBP, and FDMBP were significantly different ($p<0.05$). Although all the samples had a negative a* value (indicating greenness), the SDMBP showed a higher a* compared to other samples. The SDMBP showed a higher L* value (92.33) compared to MBF (91.87) and FDMBP (79.44). At the same time, the b* value of FDMBP (25) was found to be higher compared to MBF (22.33) and SDMBP (13.95). The lighter color of SDMBP was associated with the smaller particle size of SDMBP, which enhances the light reflectance and

Increases the lightness (Timilsena *et al.* 2016). This study also indicated that color properties were correlated to the particle size and the particle size of MBF>FDMBP>SDMBP was in association with the lower lightness color values as also found by Timilsena *et al*. (2016). Additionally, the removal of thermally unstable components in spray drying also produced a brighter color of protein powder (Dong *et al.* 2024). The findings were also supported by spray drying of protein isolates extracted from

Table 1. Functional properties of mungbean flour and protein isolates

Sample Name	S (%)	EAI (%)	ESI (min)	WHC (g/g)	OHC (g/g)	Free SH (µ mol SH/g)	Total SH (µ mol SH/g)	SS (µ mol SS/g)	T	Surface Hydrophobicity	Contact angle (°)	
											Left	Right
MBF	24.93±3.7^{a}	18.08±0.47^{a}	1.7±0.46^{a}	1.28±0.01^{a}	1.36±0.19^{a}	1.14±0.01^{a}	5.58±0.13^{a}	12.42±0.3^{a}	0.56±0.02^{a}	17.28±0.99^{a}	30.49±0.03^{a}	29.02±0.09^{a}
FDMBP	64.28±0.36^{b}	26.02±1.18^{b}	31.81±4.13^{b}	2.16±0.05^{c}	2.55±0.13^{c}	6.23±0.21^{b}	8.90±0.23^{b}	42.31±1.91^{b}	0.49±0.01^{b}	25.29±0.51^{b}	32.66±0.01^{b}	29.68±0.04^{b}
SDMBP	72.52±5.39^{c}	32.26±2.8^{c}	34.32±3.7^{b}	1.97±0.04^{b}	2.15±0.05^{b}	5.55±0.43^{c}	8.46±0.3^{b}	38.67±4.64^{b}	0.52±0.01^{ab}	30.57±0.64^{c}	39.56±0.01^{c}	40.13±0.02^{c}

Where, MBF- Mungbean flour, FDMBP- Freeze dried mungbean protein, SDMBP- Spray dried mungbean protein, S-solubility, EAI-emulsifying activity index, ESI- Emulsifying stability index, WHC- water holding capacity and OHC- oil holding capacity, SH-sulfhydryl group content, SS-Disulphide group content, T- Turbidity (The superscript a, b, c represent significant difference($p<0.05$) among the values of the same column)

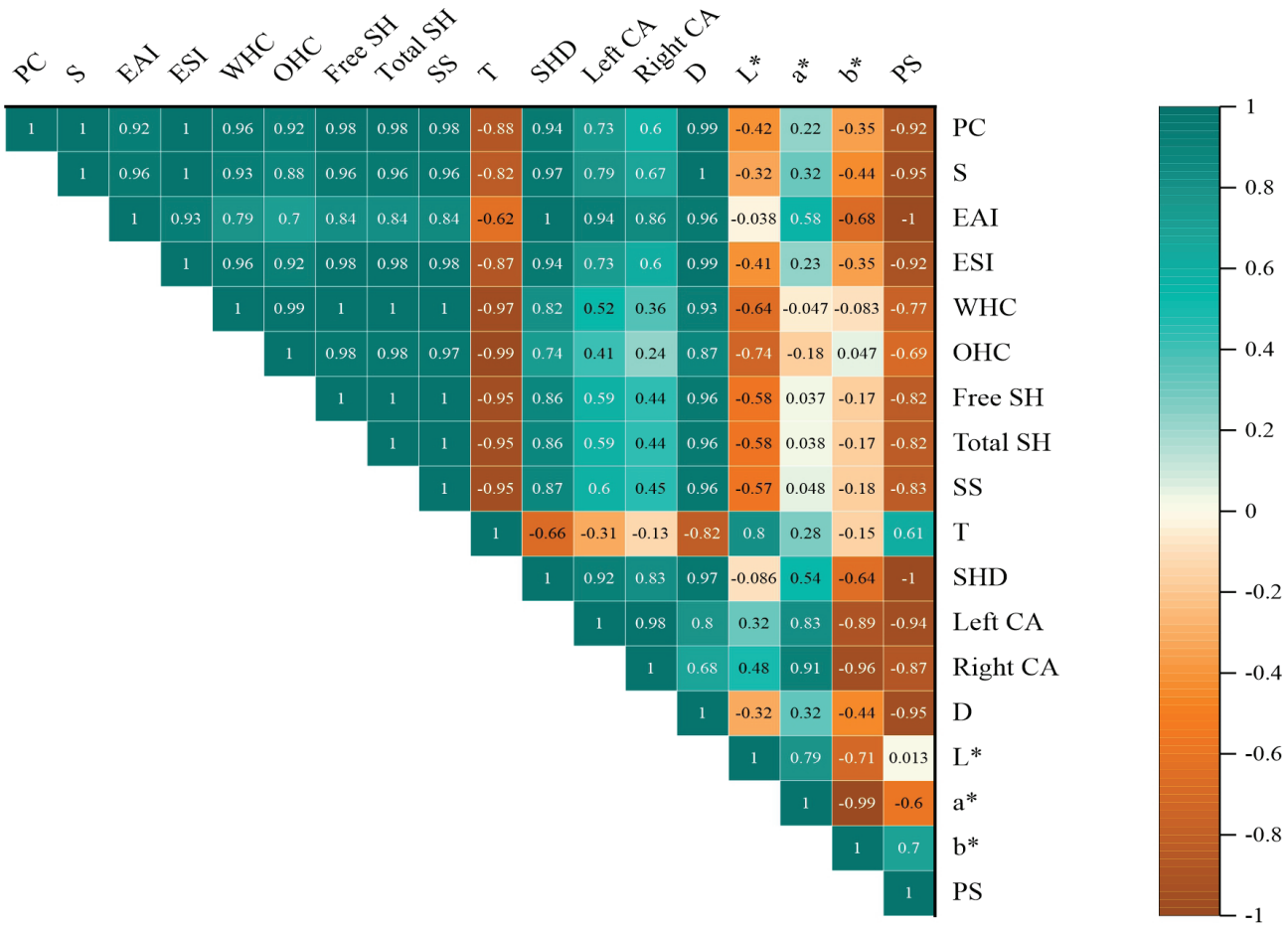

Fig. 1. Correlation between the averages of the various characteristics of the Mungbean flour (MBF), Freeze-dried Mungbean protein (FDMBP), Spray-dried Mungbean protein (SDMBP). PC indicates Protein content; S for solubility, EAI and ESI indicates Emulsifying activity index and stability index; WHC, OHC are water and holding capacities; Free SH and Total SH refers to Free and total sulfhydryl content; SS refers to the S-S group content; T refers to Turbidity; SHD refers to the Surface Hydrophobicity; Left and right CA refers to Left and Right Contact Angle; D is for Digestibility; L*, a*, and b* denote lightness/darkness, greenness, yellowness respectively; PS is Particle size.

lentil, soy, quinoa, mungbean, and chia seed (Shen *et al*. 2021, Brishti *et al.* 2020, Timilsena *et al*. 2016). Also, the high-speed homogenization before spray drying disrupts the protein tissues, heat-associated pigment denaturation, and isomerization enhances the lightness and reduces the yellowness in SDMBP (Shen *et al.* 2021). The highest yellowness of FDMBP (25) might be due to the preservation of carotenoids during freeze-drying (Wintersohle *et al.* 2023). Conclusively, factors such as particle size, composition, and pigment content diminish during drying distinctly affecting the color of the protein powder (Brishti *et al.* 2020).

Contact angle

Typically, the three-phase contact angle (θ) measures the particle wetting properties, which is crucial for determining their suitability for stabilizing different types of emulsion. Table 1 shows the contact angles of MBF (Left Contact angle (LCA) =30.49±0.03, Right Contact angle (RCA)=29.02±0.09), FDMBP (LCA= 32.66±0.01, RCA= 29.68±0.04), and SDMBP (LCA= 39.56±0.01, RCA= 40.13±0.02). In this study, all samples displayed contact angles within the range of 15° to 90°, indicating their hydrophilic nature and suitability for stabilizing oil-in-water(O/W) emulsions. SDMBP exhibited the highest contact angle, indicating a stronger affinity for the oil phase, which makes it a potential candidate for stabilizing PEs. It is generally acknowledged that the three-phase contact angle of particles between 15° and 90° exhibited a hydrophilic nature of the particle and is preferable for stabilizing the O/W emulsions, as they tend to adsorb effectively at the oil-water interface. Conversely, if the angle ranges from 90°

to 165°, the particles demonstrated a hydrophobic nature and were suitable for stabilizing water-in-oil (W/O) emulsions (Chang *et al*. 2023). The correlation analysis revealed a relationship between the contact angle (LCA and RCA) and the emulsifying properties, specifically the emulsifying activity index (EAI) and emulsifying stability index (ESI). Both LCA and RCA displayed a strong positive correlation with EAI (correlation coefficient (r) =0.94 and 0.86 respectively) and ESI (r=0.73 and 0.6 respectively), indicating that proteins with higher contact angles exhibit enhanced emulsifying capacity and stability (Figure 1). This could be attributed to the balanced hydrophilic-hydrophobic nature of proteins at the oil-water interface, which might be influenced by their wetting properties (Fameau *et al*. 2023).

Sulfhydryl and disulfide group

Sulfhydryl groups (SH) and disulfide (SS) groups are important functional groups to determine the protein's aggregation behavior and functional properties. Results showed that the SDMBP (7.55 µmol SH/g) showed the highest free groups compared to FDMBP (6.39 µmol SH/g) (Table 1). This might be associated with high-temperature spray drying induced protein unfolding which exposed more SH groups in SDMBP. The higher exposure of SH groups enhanced the protein-protein interaction, contributing to a stronger and more interconnected network within emulsions and ultimately influencing the rheological properties of emulsion. Previous studies have also reported an increase in the gel strength of protein isolate with an increase in free SH group content (Brishti *et al*. 2020). Similar results were observed for the total SH content (including both free and bound SH groups) of protein, i.e., SH bonds of SDMBP (11.46 µmol SH/g)> FDMBP (10.88 µmol SH/g). Notably, free sulfhydryl content in both proteins was higher than half of their total sulfhydryl content, suggesting more free sites available for further bonding.

SS content of protein is also useful for defining its secondary and tertiary structure. SS content of SDMBP (47.34 µmol/g) was found to be higher than FDMBP (44.31 µmol SH/g), suggesting that the spray drying promoted the formation of disulfide bonds. An increase in disulfide groups within a protein could lead to the formation of more extensive three-dimensional networks, which prohibit the protein's aggregation and exposure to hydrophobic groups (Shen *et al*. 2021). The formation of disulfide bonds and sulfhydryl group kept a balance between the exposure of hydrophobic groups and protein aggregation. An increase in the number of SS bonds in SDMBP also increased the number of covalent linkages (SS), which thus increased the emulsifying ability and stability index of the PE (Shen *et al.* 2021). Findings were also supported by Brishti et al. (2020) for drying of protein using different methods. However, the opposite findings have been reported by Gong *et al.* (2016) for the drying of peanut protein, where the SS content of FDMBP was higher than that of SDMBP. This variation in findings might be associated with the grain type, its variety, environmental stress, and protein extraction method.

Surface Hydrophobicity (Ho) measures the number of exposed hydrophobic groups in an aqueous environment and strongly correlates with the emulsifying properties of the protein. The Ho varied with the drying techniques and the highest value was observed for SDMBP (30.57) followed by FDMBP (25.29) and MBF (17.28). The highest Ho of SDMBP might be associated with high temperature-induced protein unfolding and the molecular stretching of amide bonds. This could also be explained based on the high-temperature breakdown of weak protein interactions, such as hydrogen bonding and van der Waals forces, and disrupt aggregated protein conformation. Whereas the higher Ho of FDMBP compared to MBF might be due to some degree of protein denaturation and associated exposure of hydrophobic groups. These findings demonstrate the non-severe mild denaturation effect of the optimized protein extraction method and gentle freeze-drying process on the structure of MBP isolate. Findings were positively correlated with the emulsion ability index (EAI) and supported by Feyzi *et al.* (2018).

Functional properties

The functional properties, i.e., S, EAI, ESI, WHC, and OHC of MBF and its proteins are depicted in Table 1. MBF was found to possess the lowest solubility (24.93%) among all the samples which might be due to the presence of components like starch and fiber, which hinder its solubility in aqueous solutions. However, the dried protein isolate showed higher solubility compared to MBF while the drying method significantly ($p<0.05$) varied the solubility in the protein isolate. The higher solubility of SDMBP (72.52±5.39%) compared to FDMBP (64.28±0.36%) might be due to the temperature-induced structural changes in protein treatment could cause partial denaturation and

unfolding of protein during spray drying. During spray drying, heat, exposes hydrophilic groups that enhance their interaction with water molecules and increase their solubility. Findings were also supported by Yang *et al.* (2022), who reported the higher solubility of spray dried pea protein isolate. Protein's solubility is also linked with the other properties of protein, including EAI, FC, and WHC, which play an important role in emulsion formation.

The findings of EAI and ESI reflect a material's ability to form and stabilize emulsions, which were in line with the solubility. The EAI & ESI of MBF<FDMBP<SDMBP (Table 1). The higher emulsifying properties of SDMBP were associated with the high-temperature unfolding of a globular protein and the exposure of hydrophobic amino acids. This unfolding enhanced the structural flexibility of SDMBP and allowed the diffusion of protein at the interface. This might lead to the formation of a film surrounding the oil droplets which form a stable interface (Shrestha *et al.* 2023, Brishti *et al.* 2020). Similar findings were also reported by Dahiya *et al.* (2015) and Shrestha *et al.* (2023) for mungbean flour and protein, respectively. These results suggested that the SDMBP could be used as a stabilizer in an emulsion system.

WHC and OHC of MBF were found to be 1.28 g/g and 1.36 g/g, respectively (Table 1). The WHC and OHC of protein isolates varied with the drying method, and the highest WHC (2.16 g/g) and OHC (2.55 g/g) were found for FDMBP. The higher OHC in FDMBP could be explained by the flaky and porous structure of the FDMBP sample as confirmed by SEM images (Figure 3). It increases the protein-lipid interaction via lipophilic groups and shows the superior fat-binding ability of non-polar amino acid side chains (Özdemir *et al.* 2022, Jeong and Cho 2024). In contrast to this, the lower WHC of SDMBP was attributed to the formation of moisture resistance film on the protein surface during spray drying which prevented water absorption in SDMBP. Additionally, the protein source, processing method, protein content, particle size, number of non-polar amino acids, etc., also plays an important role in the OHC and WHC of protein. Brishti *et al.* (2020) also reported the higher WHC and OHC for FDMBP isolate compared to SDMBP. They reported higher values of WHC and OHC compared to the present study. The variation in WHC and OHC might be attributed to the difference in the extraction method, different variety, and purity of protein (Brishti *et al.* 2020, Jeong and Cho 2024).

In-vitro digestibility of protein

In-vitro digestibility of protein predicts the degree of protein degradation and absorption during gastrointestinal digestion. The MBF was found to have low digestibility (76.97 %) compared to its protein isolate and the digestibility of protein isolates was non-significantly ($p>0.05$) varied with the drying method (Figure 2(A)). The highest digestibility was found in FDMBP (87.43%) followed by SDMBP (85.37%). The lower digestibility in mungbean flour compared to its protein isolate was associated with less access of the digestive enzymes to the liable peptide bonds in flour. Whereas, the denaturation process during the extraction of protein increases the accessibility of protein to digestive enzymes, which improves hydrolysis and digestibility (Barbana and Boye 2013). The slightly higher digestibility of FDMBP compared to SDMBP was mainly associated with morphological and structural differences. The FDMBP consists of a porous structure, which allows enzymes to penetrate more easily and break down the protein, while the dense structure in SDMBP could inhibit enzyme reactions and limit the protein's digestibility.

Surface morphology of proteins and flour

The SEM micrograph and surface roughness of MBF, FDMBP, and SPDMBP are shown in Figure 3. The particle morphology and roughness of MBF and protein isolates dried in spray and freeze drying were distinct from each other. The MBF particles were ellipsoidal, with the smaller number of irregular and small particles on the surface showing the highest roughness. FDMBP showed flake type and hollow non-collapsed structure with a smoother surface, whereas SDMBP showed folded and wrinkled surface morphology. The difference in morphology of both the protein isolates was mainly due to the difference in drying environment. In SDMBP, the droplets encounter hot and dry air, which shrinks the droplets due to faster moisture removal in a short drying time. Additionally, minimizing the water vapor diffusion path in high-temperature, short-time drying of protein-water droplets expedites moisture removal, resulting in wrinkled surfaces (Brishti *et al.* 2020). Whereas the porous structure of FDMBP was associated with the formation of ice crystals during freezing which subsidized freeze-drying without disturbing the structure (Zhao *et al.* 2013). There was a lack of force to break the frozen liquid into droplets during the freeze-drying evaporation process, leading to the formation of large particles and a flakey structure of

FDMBP (Chen *et al.* 2012).

FTIR analysis

The FTIR is an important tool for observing the functional groups for different wavelengths and absorbance. Figure 2D shows the functional groups present in MBF and its protein isolates dried using freeze and spray drying methods. The FTIR spectra of FDMBP and SDMBP showed characteristic bands associated with protein functional groups. The wide band at 3272 cm^{-1} corresponds to O-H stretching vibrations due to the presence of water in the sample and the N-H stretching was observed at 3069 cm^{-1} in the protein backbone. The intensity varies slightly, being more pronounced in SDMBP, potentially due to residual moisture from the drying process. The bands at 1600–1700 cm^{-1} (C=O stretching, amide I) and 1510–1580 cm^{-1} (N-H bending and C-N stretching, amide II), correspond to the major peaks for protein. Amide I portrays the strongest vibration mode, and it is important to reveal and analyze the secondary structure of the protein. These bands (amide I and II) were more pronounced in Protein isolates compared to flour, suggesting higher protein concentration in isolate compared to MBF. In MBF, these bands were still present but less intense, indicating that although MBF contains proteins, they are less concentrated or hidden by other flour components. A major change could be observed around 1000-1200 cm^{-1}, showing significant variation in absorbance. This region was typically associated with C-O stretching vibrations of carbohydrates, indicating the presence of starch or other polysaccharides in the flour sample. The disappearance of the sharp band at 989 cm^{-1} in FDMBP and SDMBP confirms that starch and sugars present only as impurities. The peak at 640 cm^{-1} in the MBF spectra suggested the presence of other molecules such as starch, fat, and other minerals. FTIR can also be used to identify changes in protein structures by detecting small shifts in band positions. However, no such shifts were observed in this study, confirming that the proteins in FDMBP and SDMBP have similar functional groups, indicating nearly identical structures (Wintersohle *et al.* 2023). Nevertheless, the higher absorbance of bands related to protein in FDMBP suggested that it had a greater protein content compared to SDMBP, which aligns with the protein content data for these samples. This slight reduction might be attributed

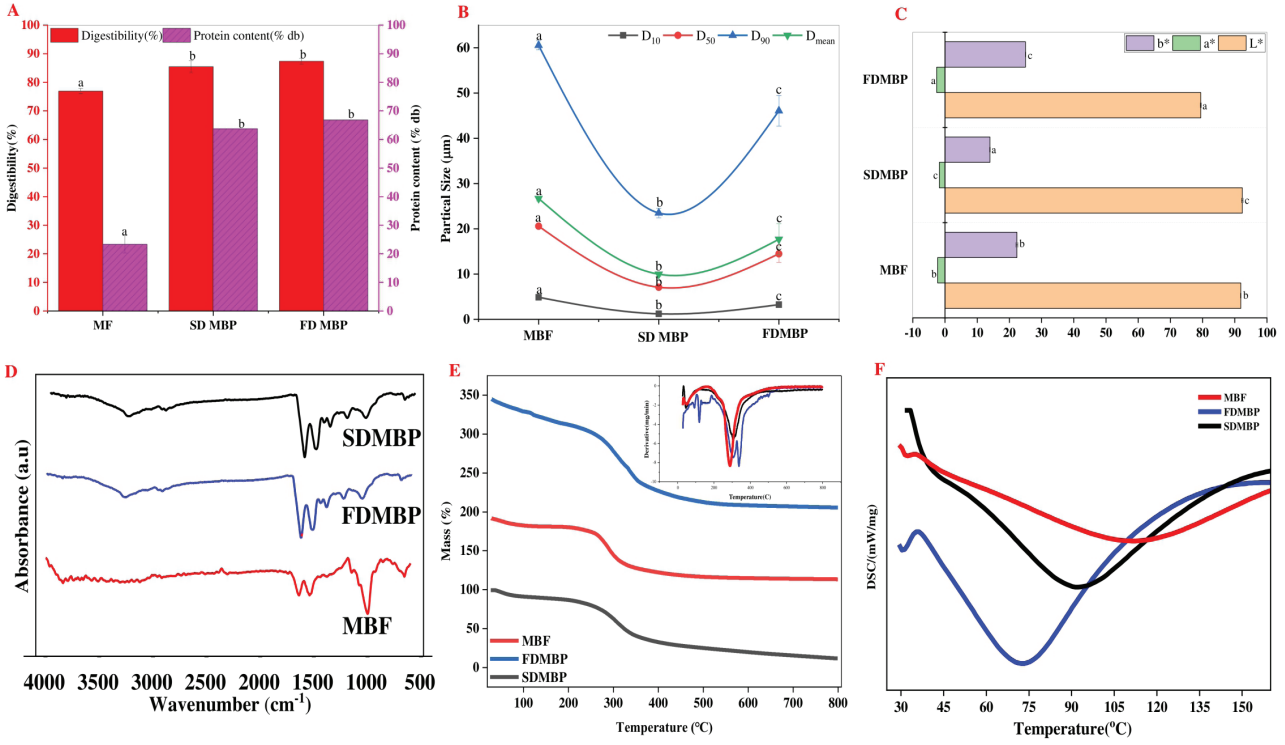

Fig. 2. Properties of MBF, FDMBP and SDMBP A) Protein content and Digestibility, B) Particle size, C) Color values, D FTIR analysis, E) Enthalpy and degradation temperature, and F) TGA thermograph (MBF- mungbean flour; SDMBP Spray dried mungbean protein; FDMBP- Freeze dried mungbean protein) (The superscript a,b,c represents significant difference ($p<0.05$) among the samples).

to protein denaturation, rapid moisture loss, and oxidation that occurred during the spray drying process (Haque and Adhikari 2015). Similar bands and findings were also reported by Ricci *et al.* (2018) for lentil, peas, chickpea, and faba bean protein isolates.

The secondary structural components of legume and pulse protein isolates, include α-helix (1650–1659 cm-1), β-sheet (1615–1640 cm-1), random coils (1641–1649 cm-1), and β-turn (1660–1688 cm-1), align well with those found in MBP, which predominantly consists of α-helix (1655–1656 cm-1), β-sheet (1625–1638 cm-1), and random coil (1641–1643 cm-1), as reported in our study (Du *et al*. 2018, Withana-Gamage *et al.* 2011). FDMBP exhibits the highest β-sheets content, and this increase promotes the exposure of hydrophobic amino acids, leading to a reduction in its solubility (Figure 4).

An increase in β-sheet promotes protein aggregation (Ventura 2005), leading to the formation of insoluble aggregates, which subsequently reduces protein solubility (Salazar-Villanea *et al.* 2016). The increase in random coil percentage suggests that some α-helix structures in FDMBP had transitioned into random coils, likely as a result of the partial

Thermal analysis

The degree of denaturation and conformational changes in protein molecules were observed using Differential Scanning Calorimetry (DSC). Denaturation temperature (Td) represents the thermal stability of the protein, and the change in enthalpy (ΔH) indicates the amount of energy required for denaturation. ΔH is the net energy required to break hydrogen bonds (endothermic) and for hydrophobic interactions (exothermic). MBF, SDMBP, and FDMBP showed distinct denaturation temperatures i.e., 100.9 °C, 107.2 °C, 153.3 °C and enthalpy (ΔH) 26.03 J/g, 24.38 J/g, 19.9 J/g, respectively (Figure 2F). MBF was found to have the highest enthalpy, while the lowest value of enthalpy was observed in FDMBP. The differences in Td and ΔH among the samples highlight the structural changes induced by the drying processes. The protein denaturation by intermolecular reactions through S-S bonds in freeze drying resulted in the reduced enthalpy of FDMBP (Dong *et al.* 2024). The lower value observed for the FDMBP sample was also attributed to the low-ordered structure of the protein and therefore reflects the amorphous structure of FDMBP formed during freeze drying (Lin *et al.* 2020). Additionally, conformational changes will likely happen during the freezing phase through the interaction between the protein and ice-water interface and the freeze concentration effect which will increase the denaturation temperature of the FDMBP (Dong *et al*. 2024). A slightly lower value

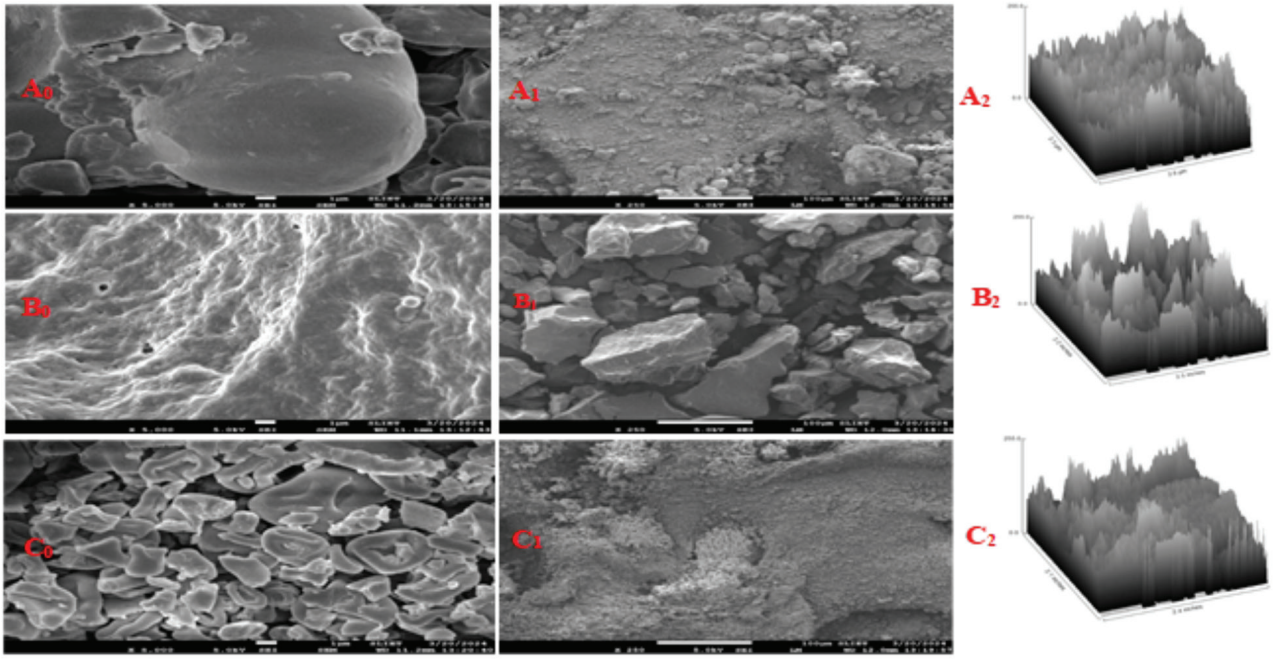

Fig. 3. SEM images and surface roughness of MBF(mungbean flour)(A_0, A_1, A_2), FDMBP (freeze dried mungbean protein) (B_0, B_1, B_2) and SDMBP (Spray-dried mungbean protein) (C_0, C_1, C_2)with magnification 5000x and 250x.

in SDMBP compared to MBF revealed denaturation of the native structure of protein during the heating process. It disrupts the hydrophobic interactions and breakdown of hydrogen bonds resulting in the formation of endothermic peaks (Yang *et al.* 2022).

The thermogravimetric analysis of MBF, FDMBP, and SDMBP is shown in Figure 2(E). The TGA curve showed weight loss with an increase in temperature, and two major weight loss were observed at 85-130 °C and 340- 370 °C. The onset (T_{onset}) and maximum degradation temperatures (T_{deg}) were obtained by plotting the first derivative of the TGA thermograph. FDMBP and SDMBP started degrading around 266 °C while MBF started degrading at 240 °C. The initial weight loss was due to the removal of the moisture present in flour and PIs. The initial weight loss in SDMBP was less compared to MBF and FDMBP, representing less moisture present in SDMBP. At the same time, FDMBP showed faster degradation in the second stage (350-360 °C) compared to SDMBP and MBF, which represents higher thermal stability of the SDMBP and flour. Both the PI were stable at high temperatures compared to MBF. The shift in decomposition temperature might be associated with the interaction of the protein with other constituents which ultimately affected the thermal behavior of the protein isolate (Ricci *et al.* 2018). Whereas the higher decomposition temperature of the protein suggested that the native structure of the protein was maintained, and the activity of the protein was preserved. These results were in accordance with the findings of Nie *et al.* (2023) for yam soluble protein.

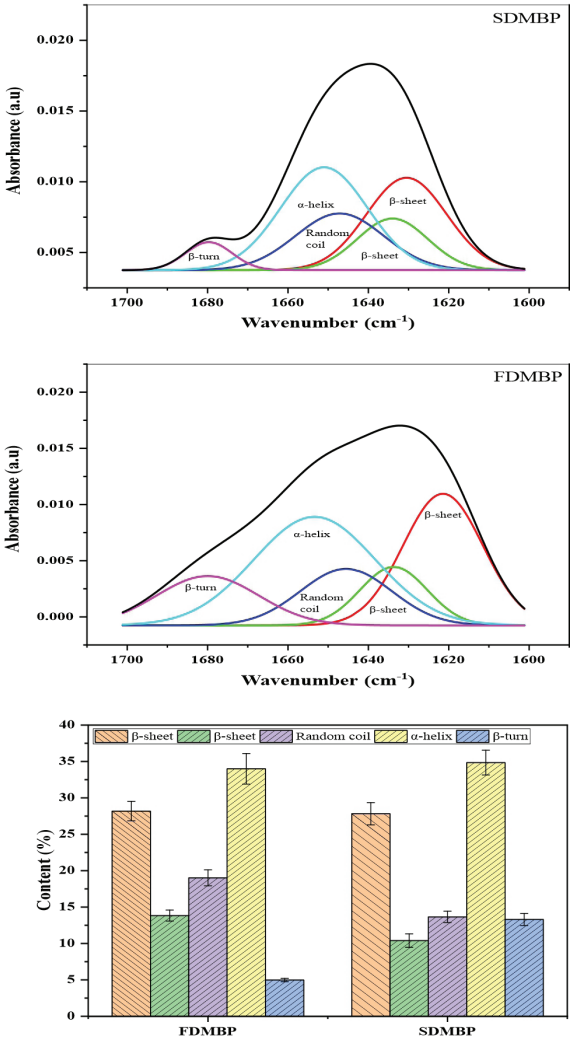

Fig. 4. Secondary structure obtained from FTIR spectrum of freeze dried (FDMBP) and spray dried (SDMBP) mungbean protein isolates

Rheological analysis of flour and protein

The rheological behavior of MBF and its PIs is shown in Figure 5. All samples exhibited shear thinning behavior, and SDMBP showed higher viscosity compared to MBF and FDMBP. The smaller particle size of SDMBP contributed to its elevated viscosity, as smaller particles have a higher surface area-to-volume ratio, leading to enhanced interactions between particles and the surrounding liquid. This observation aligns with the findings of Resch *et al.* (2004) for spray and freeze-drying of whey protein. However, beyond 80°C, G′ showed a marked increase, and the peak was observed at 95°C, which was attributed to hydrophobic interactions that play a crucial role in gel formation (Shrestha *et al.* 2023). The distinct crossover points between G′ and G′′ were identified at 93°C for MBF, 88°C for FDMBP, and 82°C for SDMBP. These crossover points correspond to the gelation temperature and the SDMBP exhibiting the lowest gelation temperature among the samples.

The variations in G′ (elastic modulus) and G′′(viscous modulus) of the MBF, FDMBP, and SDMBP during the heating and cooling processes are presented in Figure 5B. The G′ values of MBF, FDMBP, and SDMBP remained relatively consistent as the temperature rose from 25°C to 80°C. However, beyond 80°C, there was a notable increase in G′ until reaching 95°C, and no significant differences were observed during the cooling phase.

The notable increase in G′ was due to hydrophobic interaction, which played an important role in gel formation (Shrestha *et al.* 2023). A distinct

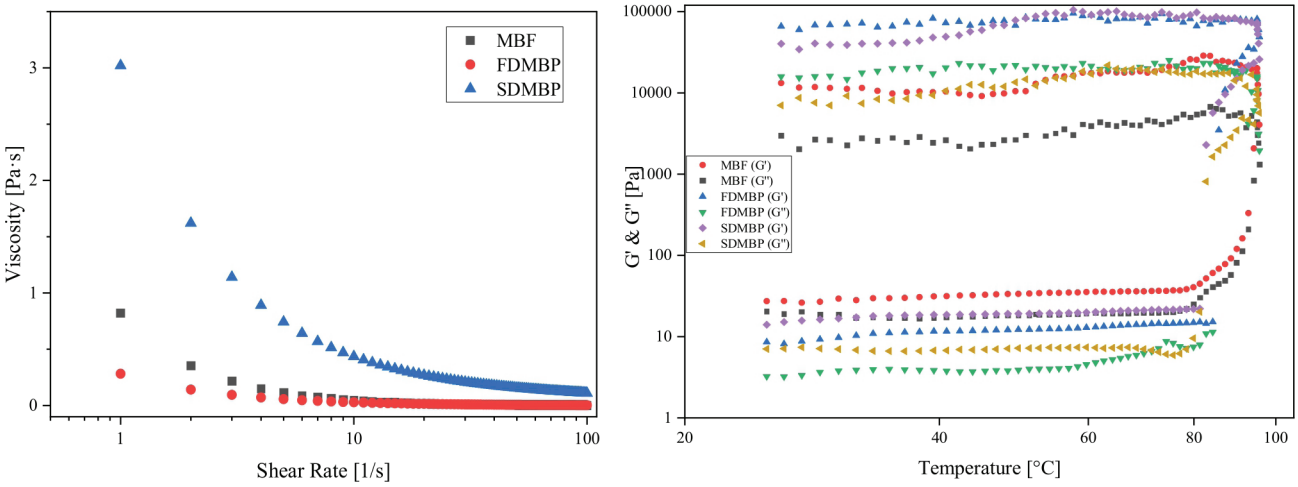

Fig. 5. Rheology of A) Viscosity vs Shear rate (proteins and flour) B) Temperature ramp (proteins and flour

crossover between G′ and G′′ was observed at 93°C for MBF, 88°C for FDMBP, and 82°C for SDMBP. This crossover point corresponds to the gelation temperature (Brishti *et al.,* 2020). These findings indicate that the gelation temperature of protein varies and depending on the drying techniques employed. Brishti *et al.* (2020) also reported a non-significant variation in the gelation temperature between FDMBP and SDMBP.

Table 2. Amino acid Profile of Freeze-dried (FDMBP) and spray-dried (SDMBP) mungbean protein isolate.

Amino acids	Freeze Dried Mung bean protein (FDMBP) (g/100g)	Spray dried Mung bean protein (SDMBP) (g/100g)
Histidine	20.6±3.4	12.5±3.1
Serine	38.7±3.7	24.9±2.4
Arginine+ Threonine	45.9±5.2	28.7±3.5
Glycine	23.2±2.6	15.5±1.6
Aspartic acid	64.7±8.2	38.6±3.2
Glutamic acid	111.9±2.4	68.8±6.2
Alanine	17.2±1.0	10.8±0.6
Proline	33±4.2	41.5±5.1
Lysine	16.7±2.1	11.2±0.4
Tyrosine	39.4±0.7	25.1±5.1
Methionine	00.5±0.0	00.8±0.1
Valine	34.1±3.2	21.8±0.3
Isoleucine	27.9±2.6	18.7±2.6
Leucine	53.1±5.3	35.3±3.1
Phenylalanine	72.1±7.2	47.5±7.1

Amino acid composition

The amino acid profiling of MBP isolates obtained through freeze drying (FDMBP) and spray drying (SDMBP) methods revealed notable differences in the composition between the two drying techniques (Table 2). Previous studies have indicated that the duration of heating significantly influences the percentage of amino acid content, with prolonged heating leading to a reduction in amino acid levels (Brishti *et al.* 2020). Freeze-drying, characterized by low-temperature processing, appears to retain a higher content of essential amino acids compared to spray-drying, which involves rapid water evaporation through the application of heat. For instance, amino acids like histidine, serine, arginine+ threonine, glycine, aspartic acid, glutamic acid, alanine, proline, tyrosine, valine, isoleucine, leucine, and phenylalanine were all present in greater quantities in the freeze-dried sample. This suggests that the MBP isolate subjected to freeze drying maintained a more robust amino acid profile, indicative of superior nutritional quality. However, both methods yield low levels of methionine, with freeze-drying marginally outperforming spray-drying in this regard. Aspartic and glutamic acids were prevalent in plant-based proteins. Both the freeze-dried (FDMBP) and spray-dried (SDMBP) samples exhibited high levels of these amino acids. Similar results were obtained by Feyzi *et al.* (2018) in their study where fenugreek protein isolates were produced using freeze drying, spray drying, and vacuum drying methods. These findings underscore the significance of processing methods in determining the nutritional value of food products, with freeze-drying emerging as a preferable technique for preserving the amino acid composition of MBP isolate.

CONCLUSION

The study explored the physicochemical and functional properties of mungbean flour (MBF) and its protein isolates obtained through freeze drying (FDMBP) and spray drying (SDMBP). Results indicated that the drying methods significantly influenced protein content, turbidity, color, particle size, and functional attributes of protein isolates. SDMBP exhibited lower turbidity, smaller particle size, and superior functional attributes compared to FDMBP and MBF. In-vitro digestibility results suggested enhanced digestibility in both SDMBP and FDMBP compared to MBF while FTIR and thermal analysis provided insights into protein structure and denaturation behavior. Rheological studies demonstrated shear thinning behavior, with SDMBP exhibiting the highest viscosity. Amino acid profiling revealed that freeze-drying emerging as a preferable technique for preserving the amino acid composition of MBP isolate. These findings were attributed to the structural changes induced by the high temperatures involved in spray drying making it suitable for various food applications such as food emulsions, plant-based milk alternatives, protein-enriched beverages, etc. Whereas higher thermal stability and amino acid preservation in FDMBP make it suitable for baked goods and high-protein snacks. Overall, these findings provide valuable insights into optimizing MBP isolates for diverse food applications.

ACKNOWLEDGMENT

All the authors are thankful to the National Institute of Food Technology Entrepreneurship and Management, Haryana, India, for infrastructural support to conduct the present study (NIFTEM-P-2024-79).

REFERENCES

Barbana C and Boye JI. 2013. In vitro protein digestibility and physico-chemical properties of flours and protein concentrates from two varieties of lentil (*Lens culinaris*). Food and Function **4**(2): 310–321.

Brishti FH, Zarei M, Muhammad S, Rashedi I, Shukri R and Saari N. 2017. Evaluation of the functional properties of mung bean protein isolate for development of textured vegetable protein. International Food Research Journal **24**(4): 1595-1605.

Brishti FH, Chay SY, Muhammad K, Ismail-Fitry MR, Zarei M, Karthikeyan S and Saari N. 2020a. Effects of drying techniques on the physicochemical, functional, thermal, structural and rheological properties of mung bean (*Vigna radiata*) protein isolate powder. Food Research International **138:** 109783.

Chao C, Park HJ and Kim HW. 2024. Effect of l-cysteine on functional properties and fibrous structure formation of 3D-printed meat analogs from plant-based proteins. Food Chemistry **439:** 137972.

Chang C, Li X, Zhai J, Su Y, Gu L, Li J and Yang Y. 2023. Stability of protein particle based Pickering emulsions in various environments: Review on strategies to inhibit coalescence and oxidation. Food Chemistry: X **18:** 100651.

Chen C, Chi YJ and Xu W. 2012. Comparisons on the Functional Properties and Antioxidant Activity of Spray-Dried and Freeze-Dried Egg White Protein Hydrolysate. Food and Bioprocess Technology **5**(6): 2342–2352.

Dahiya PK, Linnemann AR, Van Boekel MAJS, Khetarpaul N, Grewal RB and Nout MJR. 2015a. Mung Bean: Technological and Nutritional Potential. Critical Reviews in Food Science and Nutrition **55**(5): 670–688.

Dong X, Woo MW and Quek SY. 2024. The physicochemical properties, functionality, and digestibility of hempseed protein isolate as impacted by spray drying and freeze drying. Food Chemistry **433:** 137310.

Fameau AL, Guzmán E, Ritacco HA and Saint-Jalmes A. 2023. Interfacial properties of protein particles at fluid/fluid interfaces and relationship with the stability of foams and emulsions. Frontiers in Soft Matter **3**: 1016061.

Feyzi S, Varidi M, Zare F and Varidi MJ. 2018. Effect of drying methods on the structure, thermo and functional properties of fenugreek (*Trigonella foenum graecum*) protein isolate. Journal of the Science of Food and Agriculture **98**(5): 1880–1888.

Gong KJ, Shi AM, Li HZ, Liu L, Hu H, Adhikari B and Wang Q. 2016. Emulsifying properties and structure changes of spray and freeze-dried peanut protein isolate. Journal of Food Engineering **170:** 33–40.

Haque MA and Adhikari B. 2015. Drying and denaturation of proteins in spray drying process. Handbook of Industrial Drying **33**(10): 971-985

Jeong MS and Cho SJ. 2024a. Effect of pH-shifting on the water holding capacity and gelation properties of mung bean protein isolate. Food Research International **177:** 113912.

Kamboj A, Sahil, Chopra R and Prabhakar PK. 2024. Perilla protein isolate exhibits synergistic techno-functionality through modification via sequential dynamic high-pressure microfluidization and enzymatic hydrolysis. Innovative Food Science & Emerging Technologies **94:** 103683.

Kou X, Zhang X, Ke Q and Meng Q. 2023. Pickering emulsions stabilized by β-CD microcrystals: Construction and interfacial assembly mechanism. Frontiers in Nutrition **10:** 1161232.

Kudre TG, Benjakul S and Kishimura H. 2013. Comparative study on chemical compositions and properties of protein isolates from mung bean, black bean and bambara groundnut. Journal of the Science of Food and Agriculture **93**(10): 2429–2436.

Li N, Wang Y, Gan Y, Wang S, Wang Z, Zhang C, and Wang Z. 2022. Physicochemical and functional properties of protein isolate recovered from Rana chensinensis ovum based on different drying techniques. Food Chemistry **396:** 133632.

Lin N, Liu B, Liu Z and Qi T. 2020. Effects of different drying methods on the structures and functional properties of phosphorylated Antarctic krill protein. Journal of Food Science **85**(11): 3690–3699.

Nahimana P, Bouaicha I, Chèné C, Karamoko G, Missbah El Idrissi M, Bakhy K, Abdelmoumen H, Blecker C and Karoui R. 2024. Physico-chemical, functional, and structural properties of un-defatted, cold and hot defatted yellow lupin protein isolates. Food Chemistry **437:** 137871.

Nie H, Dong H, Chen Y, Hao M, Chen J, Tang Z, Liu Q, Li J, Xu X and Xue Y. 2023a. Effects of spray drying and freeze drying on the structure and emulsifying properties of yam soluble protein: A study by experiment and molecular dynamics simulation. Food Chemistry **409:** 135238.

Özdemir EE, Görgüç A, Gençdağ E and Yılmaz FM. 2022a. Physicochemical, functional and emulsifying properties of plant protein powder from industrial sesame processing waste as affected by spray and freeze drying. LWT **154:** 112646.

Resch JJ, Daubert CR and Allen Foegeding E. 2004. A comparison of drying operations on the rheological properties of whey protein thickening ingredients. International Journal of Food Science & Technology **39**(10): 1023–1031.

Ricci L, Umiltà E, Righetti MC, Messina T, Zurlini C, Montanari A, Bronco S and Bertoldo M. 2018. On the thermal behavior of protein isolated from different legumes investigated by DSC and TGA. Journal of the Science of Food and Agriculture **98**(14): 5368–5377.

Ritchie H, Rosado P and Roser M. 2022. Environmental Impacts of Food Production. Our World in Data: https://ourworldindata.org/

Sá AGA, Moreno YMF and Carciofi BAM. 2020. Plant proteins as high-quality nutritional source for human diet. Trends in Food Science & Technology **97:** 170–184.

Shen L, Li J, Lv L, Zhang L, Bai R, Zheng T and Zhang Q. 2021. Comparison of functional and structural properties of ginkgo seed protein dried by spray and freeze process. Journal of Food Science and Technology **58**(1): 175–185.

Shen Y, Tang X and Li Y. 2021a. Drying methods affect physicochemical and functional properties of quinoa protein isolate. Food Chemistry **339:** 127823.

Shrestha S, Hag, L van 't, Haritos V and Dhital S. 2023. Rheological and textural properties of heat-induced gels from pulse protein isolates: Lentil, mungbean and yellow pea. Food Hydrocolloids **143:** 108904.

Tan L, Hong P, Yang P, Zhou C, Xiao D and Zhong T. 2019. Correlation Between the Water Solubility and Secondary Structure of Tilapia-Soybean Protein Co-Precipitates. Molecules **24**(23): 4337.

Timilsena YP, Wang B, Adhikari R and Adhikari B. 2016. Preparation and characterization of chia seed protein isolate–chia seed gum complex coacervates. Food Hydrocolloids **52:** 554–563.

Wintersohle C, Kracke I, Ignatzy LM, Etzbach L and Schweiggert-Weisz U. 2023. Physicochemical and chemical properties of mung bean protein isolate affected by the isolation procedure. Current Research in Food Science **7**: 100582.

Withana-Gamage TS, Wanasundara JP, Pietrasik Z and Shand PJ. 2011. Physicochemical, thermal and functional characterisation of protein isolates from Kabuli and Desi chickpea (*Cicer arietinum* L.): A comparative study with soy (*Glycine max*) and pea (*Pisum sativum* L.). Journal of the Science of Food and Agriculture **91**(6): 1022–1031.

Ventura S. 2005. Sequence determinants of protein aggregation: Tools to increase protein solubility. Microbial Cell Factories **4**(1): 11.

Yang J, Mocking-Bode HCM, van den Hoek IAF, Theunissen M, Voudouris P, Meinders MBJ and Sagis LMC. 2022. The impact of heating and freeze or spray drying on the interface and foam stabilising properties of pea protein extracts: Explained by aggregation and protein composition. Food Hydrocolloids **133:** 107913.

Yang M, Li N, Tong L, Fan B, Wang L, Wang F and Liu L. 2021. Comparison of physicochemical properties and volatile flavor compounds of pea protein and mung bean protein-based yogurt. LWT **152:** 112390.

Zhao Q, Xiong H, Selomulya, C, Chen XD, Huang S, Ruan X, Zhou Q and Sun W. 2013. Effects of Spray Drying and Freeze Drying on the Properties of Protein Isolate from Rice Dreg Protein. Food and Bioprocess Technology **6**(7): 1759–1769.